Period-doubling route to chaos in a semiconductor laser with weak optical feedback

Jun Ye, Hua Li, and John G. McInerney
Optoelectronic Device Physics Group, Center for High Technology Materials, University of New Mexico, Albuquerque, New Mexico 87131
(Received 25 October 1991; revised manuscript received 13 March 1992)

We report experimental and theoretical observations of a period-doubling route to chaos in a semiconductor laser with optical feedback. Increasing the feedback produces a quasiperiodic route to chaos, manifested as a catastrophic increase in the laser linewidth. Under certain conditions, frequency locking occurs in preference to quasiperiodicity, and then period doubling appears. Both phenomena are explained as interactions between the external cavity modes and the laser relaxation oscillations.

PACS number(s): 42.50.Tj, 05.45.+b, 42.50.Kb, 42.55.Px

The dynamics of semiconductor lasers subject to coherent optical feedback have been studied for several years [1,2]. At low levels of feedback ($<0.1\%$ in intensity) and well above the isolated-laser threshold, increasing the feedback level initially produces linewidth narrowing, then an undamping of the relaxation oscillation followed by excitation of external cavity modes and finally a catastrophic increase in the laser linewidth, a phenomenon which has been called "coherence collapse" [1,2]. In this article we report experimental and theoretical evidence that the coherence-collapsed state is actually a chaotic one, usually obtained via a quasiperiodic route [3], but also via a period-doubling route under certain conditions. Moreover, we explain the physical basis for coherence collapse as the interaction between the external cavity modes (separated by frequency ν_{ext}) and the relaxation oscillation (ν_R) in the laser. We believe this mechanism (interaction between an external modulation and undamped relaxation oscillation) to be generally responsible for type-II laser instabilities.

Our experiments have used $GaAs/Al_xGa_{1-x}As$ laser diodes (Hitachi model HLP-1400) operating at ~ 830 nm with a single longitudinal mode. An external cavity was formed by one laser facet and a high-reflectivity plane mirror, the fraction of light coupled back being varied using a half-wave plate placed between a pair of linear polarizers, with an intracavity solid étalon of thickness 100 μm, finesse value of 30, and free spectral range ~ 1000 GHz. The ratio f_{ext} of the output intensity coupled back into the lasing mode was obtained by observing the value of f_{ext} at very weak feedback (normally $<10^{-6}$) by noting the maximum feedback-induced shift in the optical frequency [4]. Optical spectra were measured using three scanning Fabry-Pérot interferometers with free spectral ranges of 2150, 16.1, and 0.750 GHz and finesses of 300, 100, and 300, respectively. The laser intensity-noise spectra were measured using a fast *p-i-n* photodiode coupled to a microwave spectrum analyzer.

Initially the laser was biased in the range $(1.5-1.7)\,I_{\text{th}}$, the external cavity length as chosen such that the relaxation oscillation frequency was an integer multiple of the external cavity mode spacing, and the external feedback ratio was increased gradually. Figure 1 shows intensity-noise spectra near the relaxation oscillation resonance for increasing f_{ext} with $\nu_{\text{R}}=6\nu_{\text{ext}}$: the free-running laser (with $f_{\text{ext}}=0$) has damped relaxation oscillation which becomes undamped with increasing feedback. Strong features spaced by ν_{ext} also emerge, indicating the presence of multiple external cavity modes. With further increase of f_{ext}, a series of period-doubling bifurcations occurs marked by the appearance of peaks separated by $\nu_{\text{ext}}/2$ and $\nu_{\text{ext}}/4$. This process is confirmed by observation of the optical spectra, showing pronounced asymmetry of sidebands around the lasing mode. The intensity noise spectrum in the low-frequency domain is simultaneously observed to insure that frequency locking ($\nu_{\text{R}}=n\nu_{\text{ext}}$, n an integer) is maintained. Eventually the discrete noise peaks diminish while the noise floor rises, leading to a nearly white intensity-noise spectrum, and a broadened optical spectrum characteristic of coherence collapse.

In the more general case when ν_{R} is not an integer multiple of ν_{ext}, the relaxation oscillation again becomes undamped, then external cavity mode beating occurs at ν_{ext}, followed by interaction between them, and culminating once again in a coherence-collapsed state. This scenario occurs far more frequently than the period-doubling route to chaos, which requires careful monitoring of the optical spectra and control of the laser current, temperature, and external cavity length to maintain the relationship $\nu_{\text{R}}=n\nu_{\text{ext}}$. Small changes in the pump current ($\sim 0.2\%$) or external cavity length ($\sim\frac{1}{5}$ wavelength) will degrade frequency locking and hence the pure period-doubling route to chaos is not observed: it is possible to obtain a mixture of period doubling and quasiperiodicity. However, in either case the mechanism responsible for the chaotic coherence-collapsed state is the nonlinear interaction between the relaxation oscillation and external cavity modes.

Theoretically, the system is described by rate equations for the carrier population $N(t)$ and complex optical electric field $E(t)$, the latter equation being decomposed into separate equations for the intensity $I(t)$ and phase $\phi(t)$ in the active region of the laser, with a delayed nonlinear

feedback term [4–6],

$$\frac{dI(t)}{dt}=\left[\frac{G_N[N(t)-N_0]}{[1+I(t)/I_s]^{1/2}}-\gamma_p\right]I(t)+R_{\rm sp}+\kappa[(I(t)I(t-\tau)]^{1/2}\times\cos[\omega\tau+\Phi(t)-\Phi(t-\tau)]+F_I(t)\,, \quad (1)$$

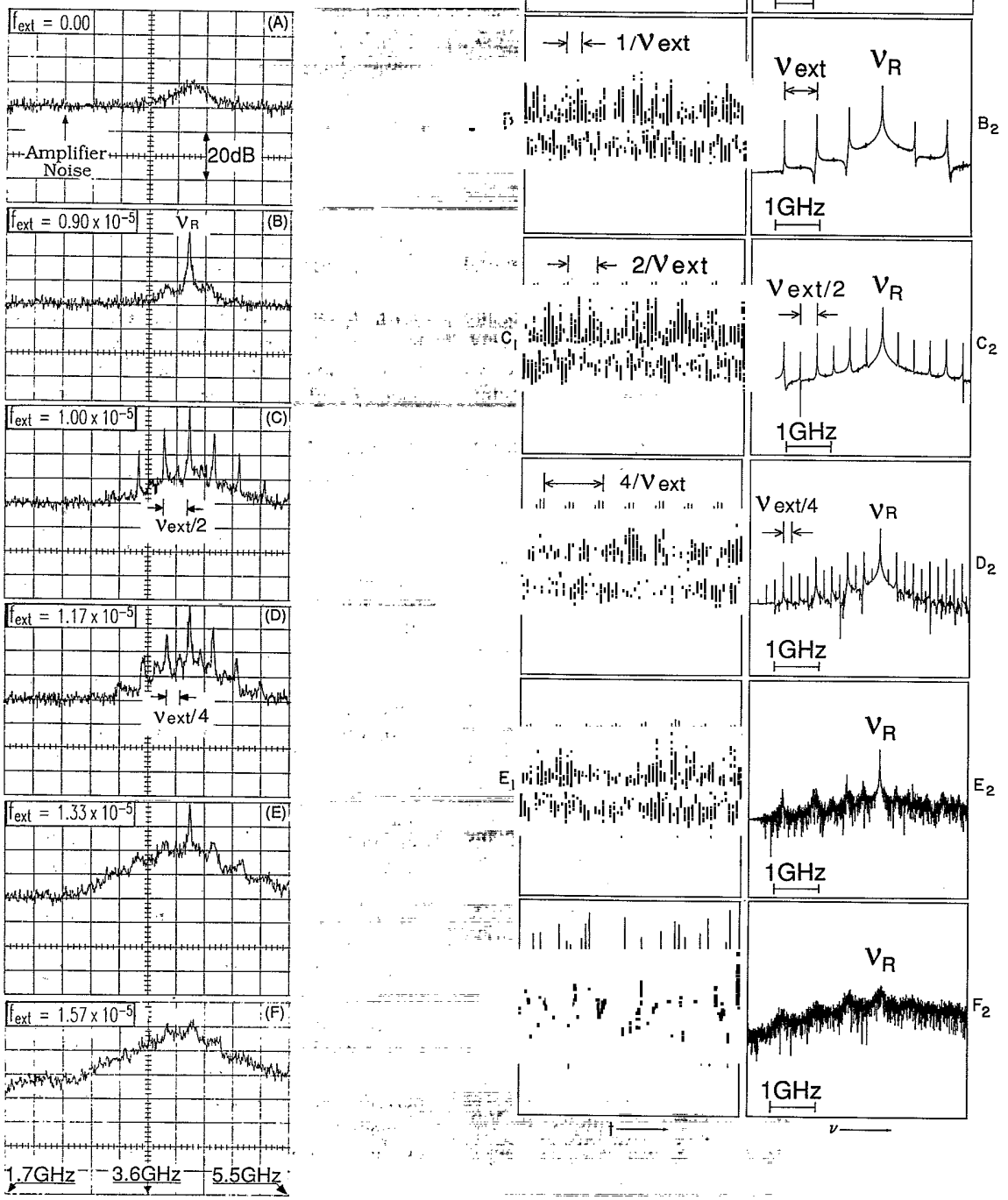

FIG. 1. Measured power spectra of the intensity with increasing feedback level $f_{\rm ext}$, when the frequency-locking condition is satisfied (A to F). The injection current $J=1.60J_{\rm th}$, the external cavity length $L_{\rm ext}=18$ cm, the external-cavity-mode spacing $\nu_{\rm ext}=0.7$ GHz, and the relaxation oscillation frequency $\nu_R=4.2$ GHz.

FIG. 2. Calculated intensity time series (first column) and power spectra (second column) for the period-doubling route to chaos as κ increases (A to F). The parameter values are $G_N=5.2\times10^3$ s^{-1}, $\gamma_p=5.8\times10^{11}$ s^{-1}, $\tau_s=3.0\times10^{-9}$ s, $N_{\rm th}=7.56\times10^8$, $N_0=6.45\times10^8$, I_s(photon numbers)$=5\times10^6$, $R=0.32$, $\tau_{LD}=7.5\times10^{-12}$ s, $\alpha=5.3$, $J=1.30\,J_{\rm th}$, and $L_{\rm ext}=18$ cm.

$$\frac{d\Phi(t)}{dt}=\frac{\alpha}{2}\{G_N[N(t)-N_0]-\gamma_p\} -\kappa\left[\frac{I(t-\tau)}{I(t)}\right]^{1/2}\sin[\omega\tau+\Phi(t)-\Phi(t-\tau)] +F_\Phi(t)\ , \tag{2}$$

$$\frac{dN(t)}{dt}=J-\frac{N(t)}{\tau_s}-\left[\frac{G_N[N(t)-N_0]}{[1+I(t)/I_s]^{1/2}}\right]I(t)+F_N(t)\ . \tag{3}$$

Here the gain rate is $G_N[N(t)-N_0]/[1+I(t)/I_s]^{1/2}$, which has included the effect of intraband relaxations of charge carriers and polarization. α is the linewidth enhancement factor. γ_p is the resonator loss rate which is equal to the threshold gain: $\gamma_p=G_{\rm th}=G_N(N_{\rm th}-N_0)$, N_0 is the value of N at transparency. J is the pump rate and τ_s is the carrier life time. $R_{\rm sp}$ is the spontaneous emission rate. $F_I(t)$, $F_\Phi(T)$, and $F_N(t)$ represent the Langevin forces of spontaneous emission noise for the intensity, phase, and carrier population, respectively. $\tau_{\rm ext}$ is the delay time of feedback and ω is the steady-state laser frequency. κ is defined as $\kappa=[(f_{\rm ext})^{1/2}(1-R)]/(\tau_{\rm LD}\cdot R^{1/2})$, where R is facet reflectivity, $\tau_{\rm LD}$ is the round-trip time of laser resonator, and $f_{\rm ext}$ is feedback coefficient of intensity. Through the feedback the phase and amplitude of the laser field are coupled. Because the phase diffusion process causes difficulties in constructing trajectories in the $\{I,\Phi,N\}$ phase space, we further transform the phase $\Phi(t)$ into the instantaneous deviation of the optical frequency from its steady-state value $\omega(t)=\lim_{\delta t\to 0}[\Phi(t)-\Phi(t-\delta t)]/\delta t$ to construct trajectories in the phase space $\{I,\omega,N\}$. We then integrate the delay-differential rate equations (1)–(3) numerically with the initial values given by the stable ready-state solution. Corresponding to the experiment case, κ is chosen as the major controlling parameter and other factors such as $\tau_{\rm ext}$ and J are varied to observe their influences on the feedback effects.

Initially, the effects of noise are not included in our calculations (Figs. 2–4). Figure 2 gives calculated time series and power spectra for the intensity $I(t)$. The time series show that the faster relaxation oscillation is initially modulated by $\nu_{\rm ext}$, then $\nu_{\rm ext}/2$, $\nu_{\rm ext}/4$, and ultimately an irregular signature. The power spectra agree well with the experimental data presented in Fig. 1. The parameter values are the same for the theory and experiment except for the feedback ratio which is a factor of five higher in the theory. The bandwidth of the spectra is limited by the linewidth of the cold laser resonator which is about 40 GHz here. The frequency spacing of external cavity modes in the power spectra is smaller than $2L_{\rm ext}/c$, due to mode pulling effects. Figure 3 shows a calculated bifurcation plot for the frequency-locked condition, showing a clear period-doubling sequence. Taking the peak values of the time series of $I(t)$ gives the envelope of the external cavity modulation signature, and taking the local maxima of this envelope gives the bifurcation points for a given $f_{\rm ext}$. However, as observed in the experiment, the quasiperiodic route occurs far more often as we vary the parameters. Frequency-locking showed the same sensitive dependence upon the controlling parameters κ, $\tau_{\rm ext}$, and J as in the experiment.

To confirm the chaotic nature of the irregular state, we calculated the correlation dimension D_2 [7] for each of the data sets in Fig. 2. The resulting data (Fig. 4) converged to a fractal dimension of 2.1–2.7, indicating a chaotic attractor. We have also calculated D_2 values for the system with white driving noise and no feedback; these values converged to 3 (with computational error $\pm$ 0.1) as expected for a purely stochastic process. The calculated value for D_2 for the coherence-collapsed state never reached 3 even with large feedback ratios and large spontaneous emission noise included. We note in passing that the uncertainties in the calculated D_2 values are due to nonuniform attractor densities caused by the stiffness of this system which has time constants ranging from $\sim$10 ps to $\sim$10 μs. The very large data set required for accurate determination of the correlation dimension D_2 precludes experimental measurements using currently available equipment. We have also studied the effects of adding realistic levels of white noise [8], indicating that

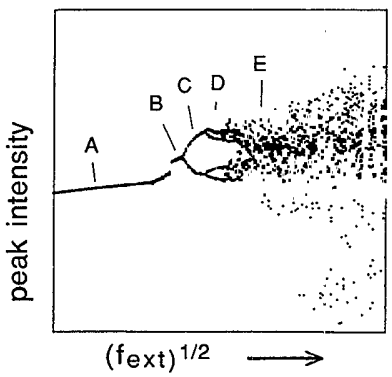

FIG. 3. Calculated bifurcation picture for the period-doubling route to chaos as κ increases. The system parameters at the points marked A to E are the same as those in the graphs similarly designed in Fig. 2.

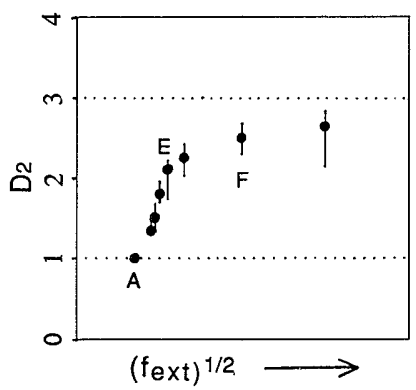

FIG. 4. Calculated correlation dimension D_2 at the points previously marked A to F during the period-doubling route to chaos.

noise causes no significant modifications of the essential features of the period-doubling or quasiperiodic routes to chaos, although it does obscure the details and make the correlation dimension more difficult to determine.

In conclusion, we have presented the first experimental and theoretical demonstration of a period-doubling route to chaos in a coherence-collapsed semiconductor laser. This route occurs in preference to the more usual quasiperiodic route when frequency-locking conditions are maintained. However, period doubling from ν_{ext} is always present even in a quasiperiodic route. In either case, the coherence-collapsed semiconductor laser is shown to be chaotic, and the behavior is due to nonlinear interaction between the external cavity modes and the relaxation oscillation undamped by the optical feedback.

The authors are grateful to N.B. Abraham and A. M. Albano at Bryn Mawr College for helpful discussions, and to the USAF Phillips Laboratory for access to a Cray-2 computer. This work was supported by the USAF Office of Scientific Research and the National Science Foundation.

[1] D. Lenstra, B. H. Verbeek, and A. J. Den Boef, IEEE J. Quantum Electron. **QE-21**, 674 (1985).

[2] G. C. Dente, P. S. Durkin, K. A. Wilson, and C. E. Moeller, IEEE J. Quantum Electron. **QE-24**, 2441 (1988).

[3] J. Mørk, J. Mark, and B. Tromborg, Phys. Rev. Lett. **65**, 1999 (1990).

[4] G. P. Agrawal and N. K. Dutta, *Long-Wavelength Semiconductor Lasers* (Van Nostrand Reinhold, New York, 1986) p. 272.

[5] R. Lang and K. Kobayaski, IEEE J. Qauntum Electron. **QE-16**, 347 (1980).

[6] G. P. Agrawal, IEEE J. Quantum Electron. **26**, 1901 (1990).

[7] P. Grassberger and I. Procaccia, Phys. Rev. Lett. **50**, 346 (1983).

[8] R. F. Fox, I. R. Gatland, R. Roy, and G. Vermuri, Phys. Rev. A **38**, 5938 (1988).